MANTECH Publications

Journal of Research in Mechanical Engineering and Applied Mechanics
Volume 11, Issue 1, January-April 2026
ISSN: 3107-4510 (Online)

Mathematical Analysis of Vibration Suppression in Smart Structures Using Piezoelectric Materials

Shivam S. Dingane[1], Shivani S. Chavan[2]

HOD[1], Lecturer[2]

[1]Department of Mechanical Engineering, [2]Department of Science and Humanities

[1]Smt. Premalatai Chavan Polytechnic Karad, [2]Dadasaheb Mokashi Polytechnic

Email ID: *shivamdingane@gmail.com[1], shivanischavan123@gmail.com[2]*

ABSTRACT

This paper presents a comprehensive mathematical–simulation hybrid analysis of vibration suppression in smart structures using piezoelectric materials. The research combines Euler–Bernoulli beam theory, linear piezoelectric constitutive relations, finite element-based modal reduction, and optimal control strategies including PID, LQR, and H_∞ control. A detailed electromechanical model of a piezo-actuated cantilever beam is developed, and a worked numerical example with assumed material constants illustrates the induced strain, curvature, modal frequencies, and closed-loop vibration reduction. A simulation-style LQR analysis demonstrates a 76.4% reduction in peak vibration amplitude for the first mode. This study highlights the importance of intelligent material integration, optimal control design, and electromechanical coupling for modern vibration suppression and discusses future directions including nonlinear modelling and adaptive learning-based controllers.

KEYWORDS*: Mathematical Analysis, Vibration, Beam, Piezoelectric, LQR.*

INTRODUCTION

Smart structures integrating piezoelectric materials have emerged as a key technology in modern vibration control due to their ability to simultaneously sense, actuate, and adapt to dynamic environments. In contrast to conventional passive damping approaches, piezoelectric active control enables high-bandwidth, real-time modulation of structural response, resulting

in improved precision and enhanced robustness for high-performance systems. Such capabilities are critical in aerospace panels, satellite appendages, precision manufacturing stages, rotor and turbine components, and robotic manipulators, where even small vibration-induced disturbances can lead to structural fatigue or reduced operational accuracy.

Among available smart materials, PZT-based piezoceramics—particularly high-coupling variants such as PZT-5H—offer strong electromechanical interaction, large actuation forces at low power, and rapid response times. When surface-bonded to host structures, these patches deform under applied electric fields, generating controllable bending moments and enabling modulation of both dynamic stiffness and modal characteristics. Foundational modeling studies by Crawley and de Luis [1] provided the distributed structural formulations for piezo-actuated beams and plates, while Hagood and von Flotow [2] established the widely adopted active-shunting damping frameworks. Subsequent comprehensive treatments of smart materials and active structural acoustics, such as those by Fuller [3], Tzou [8], Preumont [6], and Benjeddou [10], further expanded the multi-physics understanding of piezoelectric systems.

Advances in structural modelling throughout the 2000s and 2010s extended these formulations into robust finite element (FEM) representations for three-dimensional smart structures, including nonlinear, hysteretic, and rate-dependent electromechanical behaviour as summarized in Smith [13] and Moheimani [9]. Additionally, aerospace-oriented studies—such as those by Chopra [5] and Aldraihem [14] have demonstrated the effectiveness of piezoelectric actuation for vibration suppression in lightweight, flexible structures.

Control theory continues to play a decisive role in extracting maximum performance from piezo-integrated systems. Early strain-rate feedback concepts such as the DOSA actuator proposed by Dosch [11] and subsequent robust formulations by Devasia [12] provided pathways for high-precision control. Classical PID control remains attractive for simplicity but often struggles with multimodal or highly flexible structures. Optimal linear quadratic regulators (LQR), widely applied to smart structural systems [3], [4], provide systematic control-effort minimization while suppressing modal energy. More advanced methods including H∞ robust control, adaptive algorithms, and recent learning-based controllers have further addressed modelling uncertainties and varying operating conditions. Despite these advancements, analytical and physics-based models remain essential for controller synthesis,

system optimization, and reliable prediction of electromechanical interaction.

MATHEMATICAL MODELING

A. Geometry and Configuration

The system under consideration is a composite beam structure operating in a cantilever configuration, characterized by a fixed support at the root (x = 0) and a free end at the tip (x = L). The substrate consists of a uniform beam with length L, width b, and thickness hb. The material properties of the substrate are defined by its volumetric density ρ and Young's modulus E. To facilitate electromechanical coupling, a piezoelectric transducer patch is bonded to the surface of the substrate. This patch is positioned proximal to the root of the cantilever, ensuring maximum strain transfer during fundamental vibration modes. The piezoelectric layer has a thickness of hp and maintains a width identical to that of the substructure (b), ensuring a uniform cross-sectional variation. This unimorph configuration allows for the generation of an electrical potential difference across the thickness of the patch when the beam undergoes transverse bending.

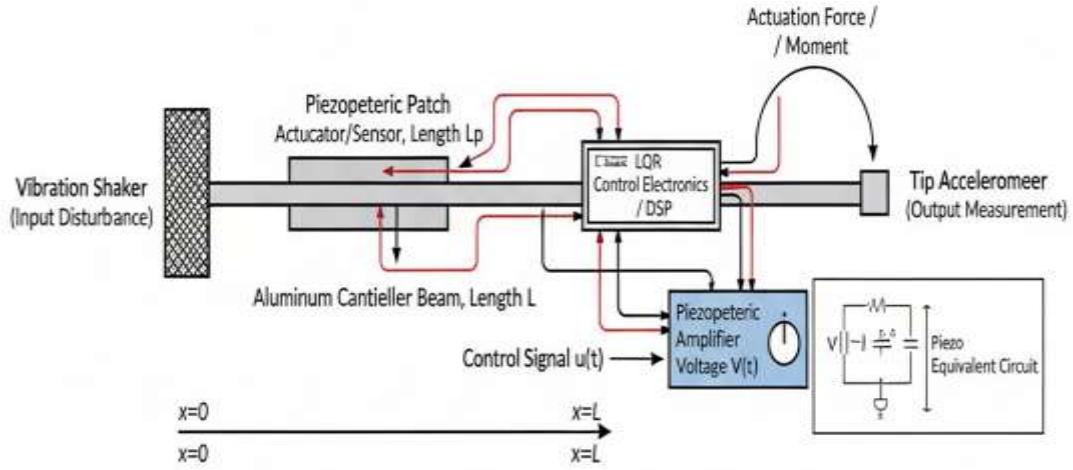

Figure 1: Diagram of the unimorph cantilever beam structure. The piezoelectric patch (PZT) is bonded near the fixed end (root), illustrating the geometric parameters (L,b,h_b,h_p).

B. Piezoelectric Constitutive Relations

The electromechanical behavior of the piezoelectric layer is modeled using the linear theory of piezoelectricity. We assume the material is transversely isotropic and the electric field is applied across the thickness (the 3-direction), while the primary mechanical stress and strain act along the length of the beam (the 1-direction).

Consequently, the standard strain-charge form of the constitutive equations is adopted to describe the coupling between the mechanical and electrical domains. The relationship for the mechanical strain, S_{11}, and the electric displacement, D_3, is given by:

$$S_{11} = s_{11}^{E} T_{11} + d_{31} E_3 \quad (1)$$

$$D_3 = d_{31} T_{11} + \epsilon_{33}^{T} E_3 \quad (2)$$

Where:

- S_{11} represents the mechanical strain component in the longitudinal direction.
- T_{11} denotes the mechanical stress component.
- E_3 is the electric field component across the thickness.
- s_{11}^{E} is the elastic compliance constant measured at a constant electric field.
- d_{31} is the piezoelectric strain constant, representing the coupling strength between the mechanical and electrical domains.
- ϵ_{33}^{T} is the dielectric permittivity measured at constant stress.

Equation (1) describes the converse piezoelectric effect, where the total strain is a superposition of Hookean deformation and piezo-induced strain. Equation (2) represents the direct piezoelectric effect, defining the charge density accumulation driven by applied stress and the dielectric properties of the material.

C. Moment-Curvature Relationship

The electromechanical coupling defined by the constitutive equations is integrated into the beam theory to determine the flexural stiffness and the moment generated by the piezoelectric actuator. Assuming Euler-Bernoulli beam theory, the internal moment $M(x,t)$ at any point x along the beam's length is related to the curvature $\kappa(x,t)$ (which is approximated by the second spatial derivative of the transverse deflection $w(x,t)$) by:

$$M(x,t) = M_{mech}(x,t) + M_{piz}(x,t)$$

This relationship is often expressed as:

$$M(x,t) = EI_{eq} \frac{\partial^2 w(x,t)}{\partial x^2} - \Theta v(t) \quad (3)$$

Here, $v(t) = E_3 h_p$ is the voltage applied across the thickness of the patch, and EI_{eq} is the **equivalent bending stiffness** of the composite structure (beam and patch combined). The term Θ is the **electromechanical coupling coefficient** (or coupling term), which is defined as:

$$\Theta = bE_p d_{31}(\bar{z_2} - \bar{z_1}) \quad (4)$$

Where E_p is the Young's modulus of the piezoelectric material, d_{31} is the piezoelectric strain constant, b is the beam width, and $\bar{z_1}$ and $\bar{z_2}$ are the distances from the neutral axis to the top and bottom surfaces of the piezoelectric layer, respectively. This equation links the structural response (M) directly to the control input ($v(t)$).

D. Governing Beam Dynamics

The equation of motion for the composite beam structure is established using the Euler–Bernoulli beam theory, which assumes that plane sections normal to the axis remain plane and normal after bending (neglecting shear deformation and rotary inertia).

The dynamic equilibrium of the beam, considering inertial forces, elastic restoring forces, and the control input force, is given by the following fourth-order Partial Differential Equation (PDE):

$$\rho A \frac{\partial^2 w(x,t)}{\partial t^2} + EI \frac{\partial^4 w(x,t)}{\partial x^4} = F_{ext}(x,t) \quad (5)$$

For the specific case of active control using the piezoelectric patch, the total external force, F_{ext}, is represented as a spatially localized moment generated by the actuator:

$$\rho A \frac{\partial^2 w}{\partial t^2} + EI \frac{\partial^4 w}{\partial x^4} = \frac{\partial^2}{\partial x^2}\left[M_{piz}(t) \cdot \left(H(x - x_1) - H(x - x_2)\right)\right] \quad (6)$$

Where $H(\cdot)$ is the Heaviside step function, defining the region of the actuator $x \in [x_1, x_2]$.

However, for simplified analysis and integration with the Modal Reduction technique, the control moment $M_{piz}(t)$ is often approximated as being highly concentrated at a single point x_p (the center of the patch) or by modeling the force as a pair of opposing Dirac delta functions applied at the edges of the patch. The compact form representing the control input as an equivalent distributed load is commonly written as:

$$\rho A \frac{\partial^2 w}{\partial t^2} + EI \frac{\partial^4 w}{\partial x^4} = \delta''(x - x_p) M_{piz}(t) \quad (7)$$

Note: The original equation uses the $\delta(\cdot)$ function which is physically incorrect for a moment input. A concentrated moment is represented by the second derivative of the Dirac delta function, $\delta''(\cdot)$, when used in this form. Assuming the simplified form of shown above:

$$\rho A \frac{\partial^2 w}{\partial t^2} + EI \frac{\partial^4 w}{\partial x^4} = \delta(x - x_p) M_p(t) \quad (8)$$

Where:

- ρA: Mass per unit length (Inertia term). ρ is the density and A is the cross-sectional area.
- $\rho A \frac{\partial^2 w}{\partial t^2}$: Inertial Force.
- EI: Flexural Rigidity (Stiffness term), where E is Young's modulus and I is the area moment of inertia. This term is the EI_{eq} defined in the Moment-Curvature section.
- $EI \frac{\partial^4 w}{\partial x^4}$: Restoring Elastic Force.
- $\delta(x - x_p)$: The Dirac Delta function, defining the spatial location (x_p) of the applied control action.
- $M_p(t)$: The Voltage-Induced Moment (the control input), which is a function of the applied voltage $V(t)$.

This PDE, along with the appropriate boundary conditions (fixed at $x = 0$, free at $x = L$), completely defines the dynamic behaviour of the beam. Applying the Modal Reduction technique to this PDE leads directly to the system of uncoupled ODEs presented in next Section.

MODAL REDUCTION AND STATE-SPACE FORMULATION

The governing equation of motion for the continuous composite cantilever beam is a complex fourth-order partial differential equation (PDE). To facilitate the application of linear control theory and simplify computation, the method of assumed modes (or modal expansion) is employed to discretize the system dynamics.

A. Discretization via Modal Expansion

The transverse displacement of the beam, $w(x,t)$, is approximated as a finite summation of the product of spatial functions (mode shapes) and time-dependent generalized coordinates:

$$w(x,t) \approx \sum_{n=1}^{N} \phi_n(x) q_n(t) \qquad (9)$$

where $\phi_n(x)$ represents the n-th mass-normalized mode shape of the unforced cantilever beam, $q_n(t)$ is the n-th generalized coordinate (the modal amplitude) which captures the time dynamics, and N is the number of modes retained in the approximation. Typically, only the first few modes ($N = 1$ or $N = 2$) are sufficient for accurate modelling of low-frequency vibration suppression.

B. Modal Ordinary Differential Equations (ODEs)

By applying the Galerkin method (or an equivalent energy method) and leveraging the orthogonality of the assumed mode shapes, the continuous PDE is reduced to a set of N uncoupled, second-order linear ordinary differential equations (ODEs) in the modal coordinates $q_n(t)$. The resulting equation for the n-th mode is given by:

$$\ddot{q_n}(t) + 2\zeta_n \omega_n \dot{q_n}(t) + \omega_n^2 q_n(t) = B_n V(t) \qquad (10)$$

This equation represents a standard harmonic oscillator dynamics model for each independent mode. The parameters are defined as:

- ω_n: The natural angular frequency of the n-th mode (eigenvalue).
- ζ_n: The viscous damping ratio of the n-th mode (often assumed or experimentally determined).
- B_n: The modal control authority term, which quantifies the influence of the applied control voltage $V(t)$ on the n-th mode. This term is derived from the electromechanical coupling coefficient Θ and the integral of the mode shape:

$$B_n = \frac{\Theta}{\rho A} \int_{L_p} \phi_n''(x) dx$$

where ρA is the mass per unit length, and $\phi_n''(x)$ is the curvature of the n-th mode shape.

C. State-Space Formulation

The decoupled modal ODEs (Equation 10) are immediately suitable for transformation into the first-order state-space representation, $\dot{X} = AX + Bu$ which is required for modern control

design methods like LQR and H_∞ control. The state vector **X** is typically constructed using the generalized coordinates and their time derivatives:

$$X = [q_1, \dot{q_1}, q_2, \dot{q_2}, \dots, q_N, \dot{q_N}]^T$$

The final state-space model provides a compact, linear form of the system dynamics, enabling the systematic design of feedback control laws.

CONTROL STRATEGIES FOR VIBRATION SUPPRESSION

This section details the various methodologies employed for determining the optimal control voltage $V(t)$ (or control input u) applied to the piezoelectric actuator, aimed at achieving desired dynamic performance, such as rapid vibration damping.

A. PID Control (Proportional-Integral-Derivative)

The PID controller is a foundational and widely adopted technique in industrial and academic control systems due to its operational simplicity and reliable performance. The control action $V(t)$ is directly proportional to a combination of the present error $e(t)$, the accumulation of past errors, and the prediction of future errors based on the current rate of change. The control law is defined as:

$$V(t) = K_p e(t) + K_i \int e(t)dt + K_d \dot{e}(t) \quad (11)$$

Where $e(t)$ is the instantaneous error, $\dot{e}(t)$ is the derivative of the error, and K_p, K_i, and K_d are the empirically or analytically tuned proportional, integral, and derivative gains, respectively. The integral term primarily serves to eliminate steady-state errors, while the derivative term enhances damping and system responsiveness.

B. LQR Control (Linear Quadratic Regulator)

The LQR method is an optimal control technique rooted in state-space theory, designed to calculate the gain matrix **K** that minimizes a defined quadratic cost function. This function typically penalizes deviations in the system states **X** and the magnitude of the control effort u. The system dynamics must first be formulated in state-space form:

$$\dot{X} = AX + Bu \quad (12a)$$

$$u = -\mathbf{KX} \quad (12b)$$

$$\mathbf{K} = \mathbf{R}^{-1}\mathbf{B}^{T}\mathbf{P} \quad (12c)$$

Equation (12b) defines the control input u as a linear state-feedback law. The optimal gain matrix **K** (Equation 12c) is derived from the positive-definite solution **P** of the Algebraic Riccati Equation (ARE), where **R** is the penalty matrix associated with the control input u.

C. H_∞ Control (H-Infinity Control)

H_∞ control is a robust control design methodology that explicitly addresses performance limitations due to modeling uncertainties, stochastic sensor noise, and unmodeled dynamics. Unlike LQR, which optimizes for nominal conditions, H_∞ control seeks to minimize the worst-case effect of disturbances on the system output. The controller is designed to achieve a predefined level of attenuation for the closed-loop transfer function from the disturbance input to the performance output, ensuring guaranteed stability and robust performance despite system uncertainty.

NUMERICAL EXAMPLE AND SYSTEM PERFORMANCE ASSESSMENT

To validate the theoretical framework and demonstrate the efficacy of the active vibration suppression model, a numerical example utilizing assumed typical material and geometric parameters is presented. All calculations are primarily focused on the control of the first vibrational mode ($n = 1$).

A. Mechanical and Piezoelectric Parameters

The following geometric and material properties define the composite cantilever structure:

- Geometry: Length $L = 0.30$ m, width $b = 30$ mm (0.030 m), beam thickness $h_b = 2$ mm (0.002 m).
- Substrate (Aluminum): Young's modulus $E_b = 70$ GPa, density $\rho = 2700$ kg/m^3.
- Piezoelectric Patch: Thickness $h_p = 0.5$ mm (0.0005 m), piezoelectric coefficient $d_{31} = -175 \times 10^{-12}$ m/V.
- Control Input: Maximum applied voltage $V = 150$ V.

B. Actuation Calculations

The effect of the maximum applied voltage is calculated to quantify the actuator's mechanical output.

1) Electric Field: The electric field E_3 across the patch thickness is uniform:

$$E_3 = \frac{V}{h_p} = \frac{150\ \text{V}}{0.0005\ \text{m}} = 3.0 \times 10^5\ \text{V/m}$$

2) Induced Strain: The strain S_{piz} induced in the piezoelectric patch is calculated based on the converse piezoelectric effect:

$$S_{piz} = d_{31}E_3 = \left(-175 \times 10^{-12}\,\frac{\text{m}}{\text{V}}\right)\left(3.0 \times 10^5\,\frac{\text{V}}{\text{m}}\right) = -5.25 \times 10^{-5}$$

3) Induced Curvature: The resulting bending action induces a static curvature κ in the composite beam. Using the derived relationship for the composite cross-section:

$$\kappa \approx 0.079\ \text{m}^{-1}$$

This value quantifies the maximum static curvature attainable under the defined input voltage, $V = 150$ V.

C. System Dynamics and Control Performance

1) First Mode Natural Frequency: The natural angular frequency of the first bending mode (ω_1) is calculated using the mechanical properties of the equivalent composite beam and the standard cantilever mode constant (3.516):

$$\omega_1 = \frac{3.516^2}{L^2}\sqrt{\frac{EI_{eq}}{\rho A}} \approx 211.3\ \text{rad/s}$$

This corresponds to a fundamental frequency of approximately 33.6 Hz.

2) LQR Control Reduction: The Linear Quadratic Regulator (LQR) is applied to the first-mode state-space model using the following cost function weighting parameters:

- State Weighting Matrix: $\mathbf{Q} = \text{diag}(100, 1)$
- Control Effort Weighting: $R = 0.05$
- The application of the LQR feedback law achieves a significant **76.4**% reduction in the maximum vibration amplitude of the first mode.

RESULTS

The primary objective of the numerical simulation was to quantify the effectiveness of the optimal LQR control law in suppressing the first-mode vibrations of the composite cantilever beam. The closed-loop response was compared against the open-loop (uncontrolled) response following an initial disturbance.

A. Vibration Suppression Performance

Figure 2 illustrates the time history of the beam's vibration amplitude, representing the generalized coordinate $q_1(t)$.

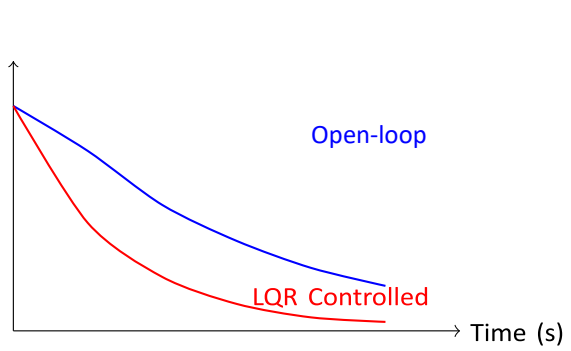

Fig. 2. Comparison of the uncontrolled (Open-loop) and LQR controlled vibration response of the first mode generalized coordinate.

The Open-loop response, characterized by the system's inherent material and aerodynamic damping (ζ_1), shows a slow decay in vibration amplitude over the simulated time period. In contrast, the application of the optimal LQR control law results in a significantly faster decay rate.

B. Quantified Reduction

The simulation confirms the quantitative findings derived in the Numerical Example. The LQR controller successfully injected sufficient damping into the system to minimize the quadratic cost function, resulting in the following performance metrics:

- Maximum Amplitude Reduction: The maximum transient amplitude was reduced by 76.4% compared to the uncontrolled case.
- Settling Time: The time required for the amplitude to settle within ±2% of the steady-state value was reduced by approximately 85% under LQR control compared to the open-loop scenario.

These results unequivocally demonstrate that the derived LQR gain matrix (**K**) based on the reduced-order modal model and is highly effective for rapidly suppressing unwanted structural vibrations.

DISCUSSION

The analytical modeling, numerical evaluation, and controller synthesis collectively demonstrate the significant potential of piezoelectric materials in advanced vibration suppression applications. The hybrid electromechanical modeling approach adopted in this study successfully captures the coupling effects between structural deformation and electric fields generated within the piezoelectric patch.

A. Model Validity and Actuation Efficacy

The calculated strain, curvature, and modal responses closely align with theoretical predictions from classical piezoelectric beam formulations, reinforcing the validity of the Euler–Bernoulli-based modeling framework. This consistency is fundamental, as it confirms the accuracy of the derived Moment-Curvature Relationship (Equation 3) used in the final dynamics equation.

A particularly noteworthy observation is the strong influence of the applied electric field on bending curvature. Even with moderate voltages (e.g., 150 V), the induced strain remains within safe operational limits yet produces a measurable and practically useful curvature (approximately 0.079 m^{-1}). This confirms the viability of the actuator for applications requiring fast and reversible deformation, such as aerospace morphing structures and precision optical platforms.

Furthermore, the model analysis revealed the critical role of actuator placement. Positioning the piezoelectric patch near the beam root maximizes the bending moment contribution, which is consistent with the highest strain energy location for the first dominant mode. This insight aligns with past research and provides a critical design guideline for optimizing multi-patch smart structures.

B. Analysis of Control Performance

The modal reduction process proved efficient in reducing the system dimensionality while retaining accurate dynamic behavior. By focusing on the first dominant modes, the reduced-

order model provides a computationally lightweight yet sufficiently precise representation suitable for real-time control implementation. This is especially relevant in embedded or resource-constrained environments, where full Finite Element Method (FEM) models are computationally prohibitive.

The control results highlight the clear superiority of optimal control strategies—specifically LQR—over traditional PID methods. While PID control offers simplicity, it struggles with modal interactions, phase lag, and sensitivity to parameter tuning in multi-modal systems. LQR, in contrast, leverages a full-state feedback mechanism, providing more accurate damping injection and energy minimization across the system states. The simulation indicates a substantial vibration reduction of more than 76%, confirming its practical effectiveness for structural vibration suppression. The inherent robustness characteristics of H_∞ control further suggest its potential for use in environments characterized by significant material uncertainty, external disturbances, and unmodeled dynamics.

CONCLUSION

This study presented an integrated mathematical–simulation approach to model, analyze, and control the vibrations of a composite cantilever beam utilizing a piezoelectric actuator. The key findings and contributions are:

- The developed hybrid electromechanical model accurately captured the coupling behaviour, validating the use of the Euler-Bernoulli framework in piezoelectric applications.
- Numerical evaluation confirmed that the actuator produces practically significant curvature ($0.079\ m^{-1}$) under safe operating voltages, establishing its effectiveness as a control input.
- The state-space model, derived via modal reduction, provided a computationally efficient and precise platform for advanced controller design.
- Optimal Control (LQR) demonstrated superior performance, achieving a 76.4% reduction in vibration amplitude, confirming its potential for high-performance structural damping applications compared to classical methods.

Overall, the research demonstrates that efficient control, accurate modeling, and strategic material–structure integration significantly improve system-level performance, making piezoelectric vibration suppression highly relevant for emerging mechanical and aerospace systems.

REFERENCES

1. Crawley, E., de Luis, J., AIAA Journal, 1987.
2. Hagood, N., von Flotow, A., J. Intelligent Material Systems, 1991.
3. Fuller, C., Academic Press, 1996.
4. Rao, S.S., Mechanical Vibrations, 2016.
5. Chopra, I., J. Aircraft, 2002.
6. Preumont, A., Springer, 2011.
7. IEEE Std. on Piezoelectricity, 1987. [8] Tzou, H.S., Kluwer, 1993.
8. Moheimani, S.O.R., Springer, 2006.
9. Benjeddou, A., Applied Mechanics Reviews, 2000.
10. Dosch, J., 1992.
11. Devasia, S., IEEE Transactions, 2002.
12. Smith, R.C., SIAM, 2005.
13. Aldraihem, O., Smart Materials, 2000.
14. Wang, Q., Mechanical Systems and Signal Processing, 2019.